Supplementary Information

Supplementary Figures
Figure S1

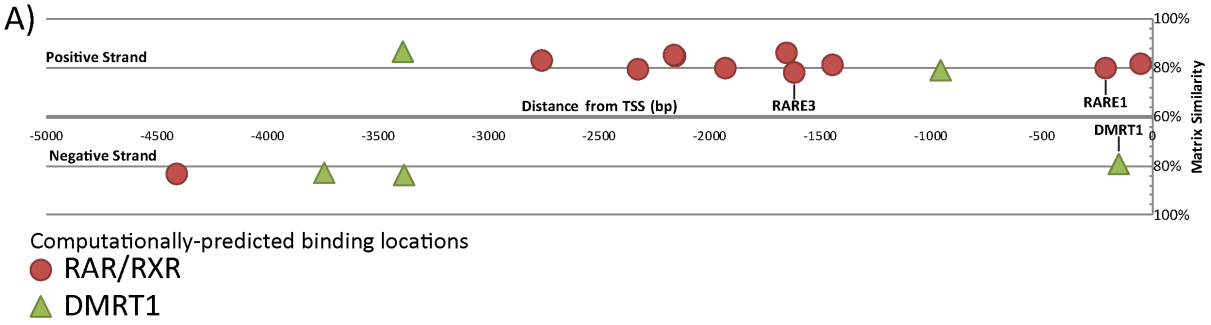

Transcription Factor Matrix	Start position	End position	Strand	Matrix sim.	Sequence
Retinoic acid receptor / retinoid X receptor heterodimer	-4418	-4394	-	0.833	AGGAGGATCGTTGCCAGTTCAAGAA
	-2774	-2750	+	0.831	ACTCCTCTGGCTCAGAGGTCTTTAG
	-2337	-2313	+	0.797	ACAAACCAGGACCAAAGGACATTGA
	-2176	-2152	+	0.856	CAGGGATGCGGTCATAGGCCACAGG
	-2169	-2145	+	0.852	GCGGTCATAGGCCACAGGGCATACG
	-1942	-1918	+	0.799	AAGTTCAAAGGATAGTGGTCATATG
	-1667	-1643	+	0.862	GCTGAGACCTGTCAGAGGTCAAAGT
	-1634	-1610	+	0.785	CTCCACATTCCTCACAGGTCAAGGA
	-1459	-1435	+	0.816	AGAGTCAGAAGGGATAGGTCATGAC
	-221	-197	+	0.803	CTGGATGGGGTGAAAAGGTCATCTT
	-65	-41	+	0.817	GCAGCCTGGGGTACCAGGTCAGTTT
Doublesex and mab-3 related transcription factor 1	-3754	-3734	-	0.828	GTGAGAAGGGACATTGTGGGA
	-3400	-3380	+	0.869	GTATGTTGGCACACTGTATCC
	-3394	-3374	-	0.833	GGCTGGGGATACAGTGTGCCA
	-968	-948	+	0.793	AATTTAAGGTACCCTGTTGCA
	-161	-141	-	0.789	ATTGGTGAAAACATTGTAACA

Figure S1: Computational prediction of RAR/RXR and DMRT1 binding sites 5kb upstream of *Stra8* TSS using MatInspector.

Graphical representation of the location of putative RAR/RXR (red circle) and DMRT1 (green triangle) binding sites in relation to TSS of *Stra8*. Identified binding sites on the positive strand and negative strands are shown above and below the midline respectively. Putative binding sites are called when matrix similarity is >0.75, and this is indicated by their distance away from the midline; sites further away have higher similarity scores. Binding sites corresponding to RARE1, RARE3 and DMRT1 examined in this study are also indicated.

Figure S2

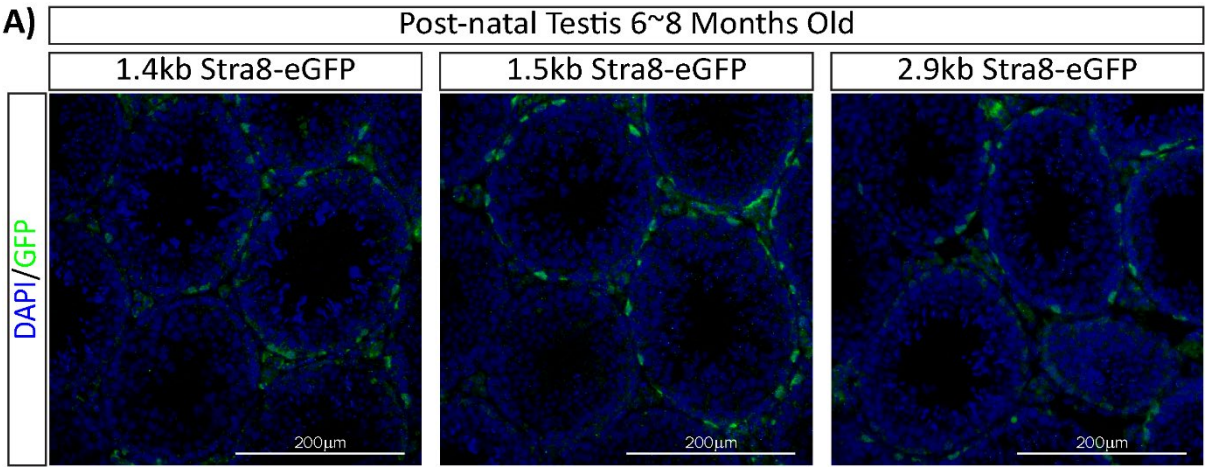

Figure S2: Testicular expression of eGFP is similar among in all three *Stra8* promoter lines. Immunofluorescent analysis of adult testis for eGFP expression shows that, in all three lines, GFP is detectable in a pattern similar to that observed in previous studies (Giuili et al., 2002; Sadate-Ngatchou et al., 2008).

Figure S3

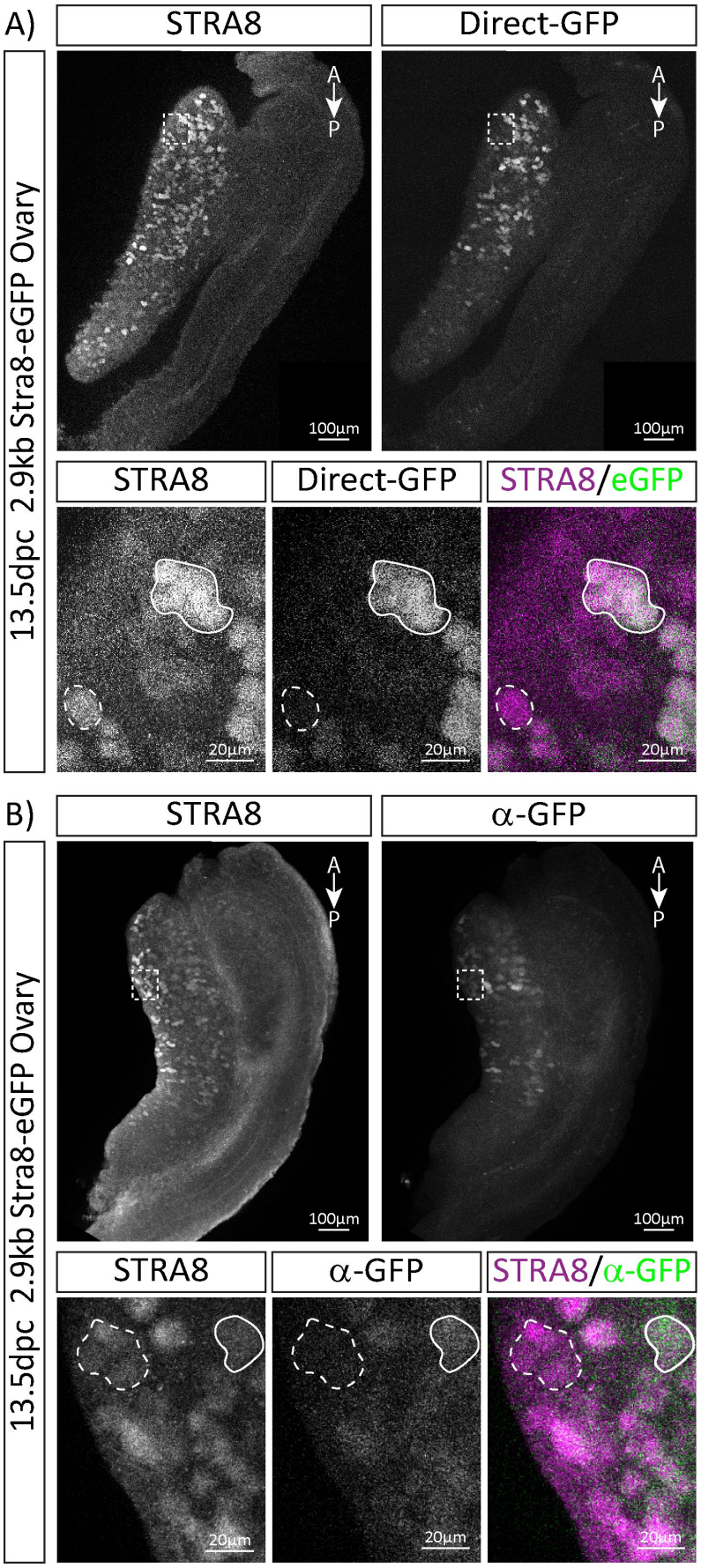

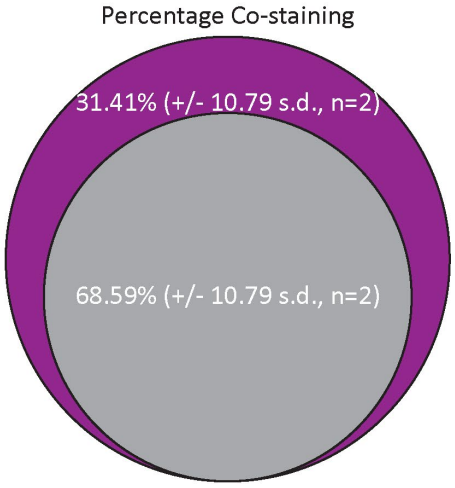

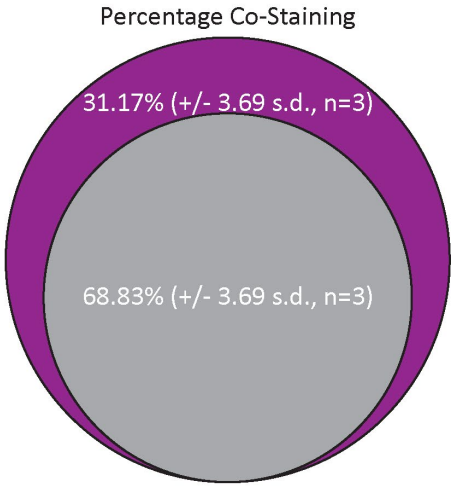

Figure S3: eGFP driven by the 2.9kb *Stra8* promoter co-localises with STRA8 protein expression in approximately 68% of germ cells.

A) Whole mount immunofluoroscence analysis of 13.5 dpc 2.9kb Stra8-eGFP ovaries stained for STRA8 expression, compared to direct eGFP signal produced. Cells co-expressing STRA8/eGFP (solid lined) accounted for 68.59% (+/- 10.79 s.d, n=2, 348 total cells counted) of total STRA8-positive cells (dotted lined). No cells expressing eGFP only were observed. B) Whole mount immunofluoroscence analysis of 13.5 dpc 2.9kb Stra8-eGFP ovaries stained for STRA8 expression, compared to anti-GFP antibody detection. Cells co-staining for STRA8/anti-GFP (solid lined) accounted for 68.83% (+/- 3.69 s.d, n=3, 653 total cells counted) of total STRA8-positive cells (dotted lined). No cells staining for GFP only were observed.

Figure S4

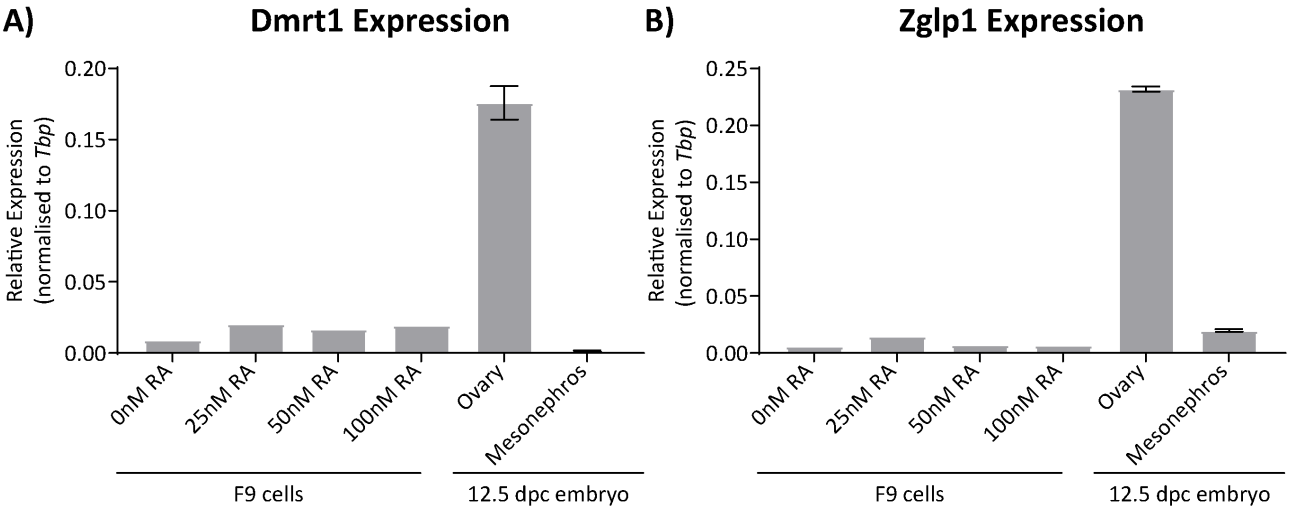

Figure S4: Lack of *Dmrt1* and *Zglp1* expression in F9 EC cells

A) *Dmrt1* is not present at appreciable levels in F9 cells and is not upregulated in response to RA, excluding a mechanism by which RA induces *Dmrt1* expression and DMRT1 drives *Stra8* expression (n = 1, see text for more detail). B) Downstream effector of BMP signalling, *Zglp1,* is not expressed in F9 cells and is not upregulated in response to RA treatment (n=1). Quantitation of expression in 12.5 dpc ovaries and mesonephros are included as positive and negative controls, respectively, for comparison (n=3).

Figure S5

Figure S5: CRISPR/Cas9 mutation strategy of RARE1 and RARE3.

A) RARE1 specific CRISPR guide RNA (RARE1sgRNA) was designed to target RARE1 (black rectangle) at -200nt relative to *Stra8* TSS. Mutataions to RARE1 are incorporated when the CRISPR/Cas9 mediated double stranded break is repaired by homology directed repair (HDR) using co-injected RARE1_ssODN as the repair template. Target sequence was mutated to also disrupt the PAM recognition sequence, to prevent CRISPR/Cas9 re-targeting of successful HDR events. We included a *SalI* restriction enzyme site to facilitate genotyping. B) RARE3 at -1613nt was targeted for mutation using a similar strategy as for RARE1. C) An unplanned non-homologous end joining repair by-product of targeting RARE1 generated the mutant line Δ173bp, where sequence between -55 and -228nt upstream of *Stra8* TSS (encompasing RARE1 and DMRT1 binding sites) was deleted.

Previously identifed RARE2 and a TATA-box like sequence remained intact. The Δ173bp is effectively a *Stra8*-null mouse line as both sexes are infertile.

Figure S6

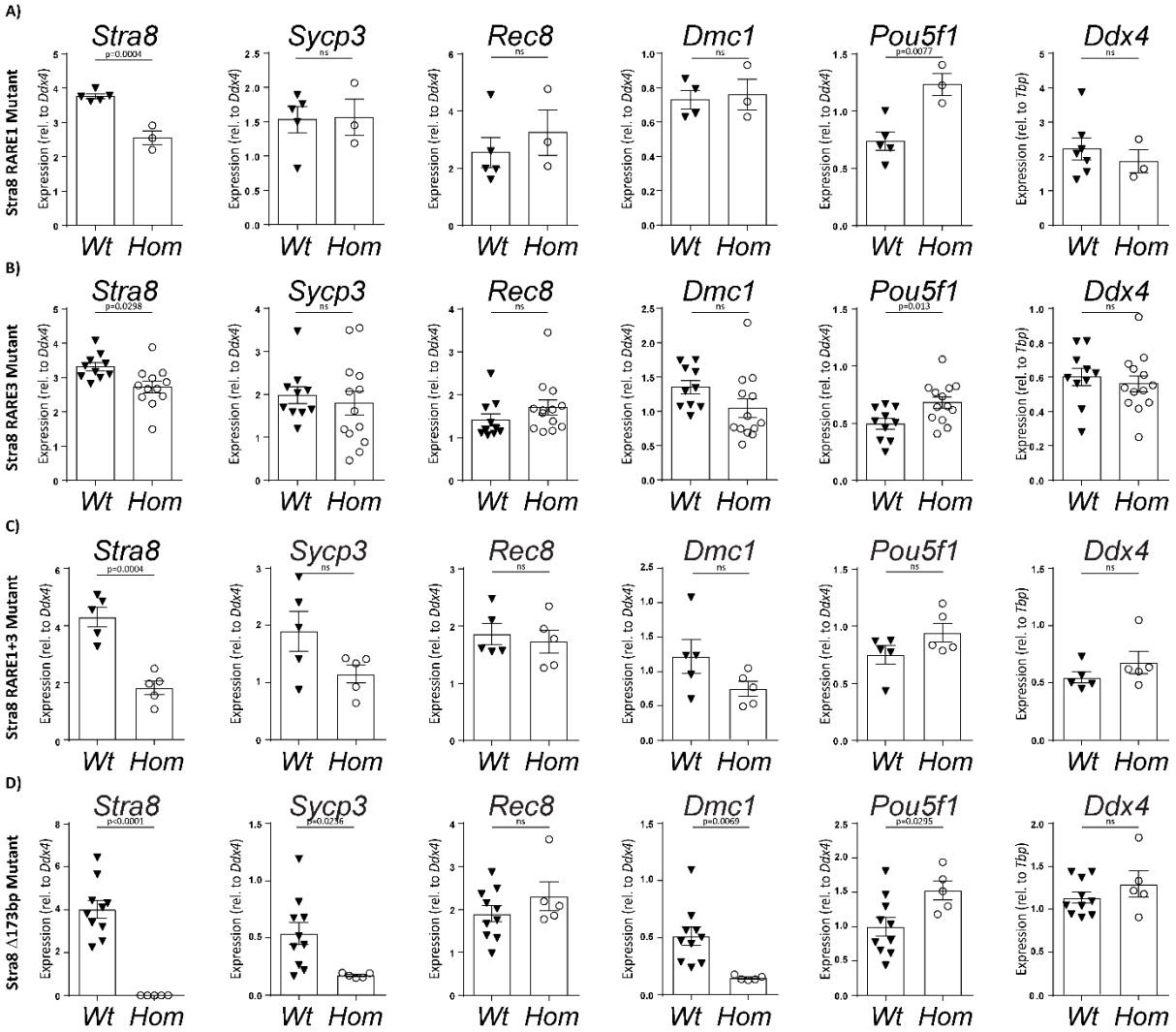

Figure S6: Meiotic and germ cell gene expression in 14.5 dpc fetal ovaries of the CRISPR/Cas9 mutant mouse lines compared to wildtype littermates.

A-C) RARE1, RARE3 and RARE1/3 mutant lines all show decreased *Stra8* expression by qRT-PCR, however other meiotic markers are not significantly perturbed. Importantly *Rec8*, another RA reponsive gene, is unaffected indicating the decrease in *Stra8* expression is not due to lower levels of RA. Retention of *Pou5f1* expression is observed at varying degrees of magnitude. D) In the Δ173bp mutant there is no detectable expression of *Stra8* and expression of later stage meiotic markers *Sycp3* and *Dmc1* is substantially diminished. *Rec8* expression is not significantly altered in RARE1, RARE3 or RARE1/3 lines, as expected (mean ± s.e.m, t-test, n > 3).

Figure S7

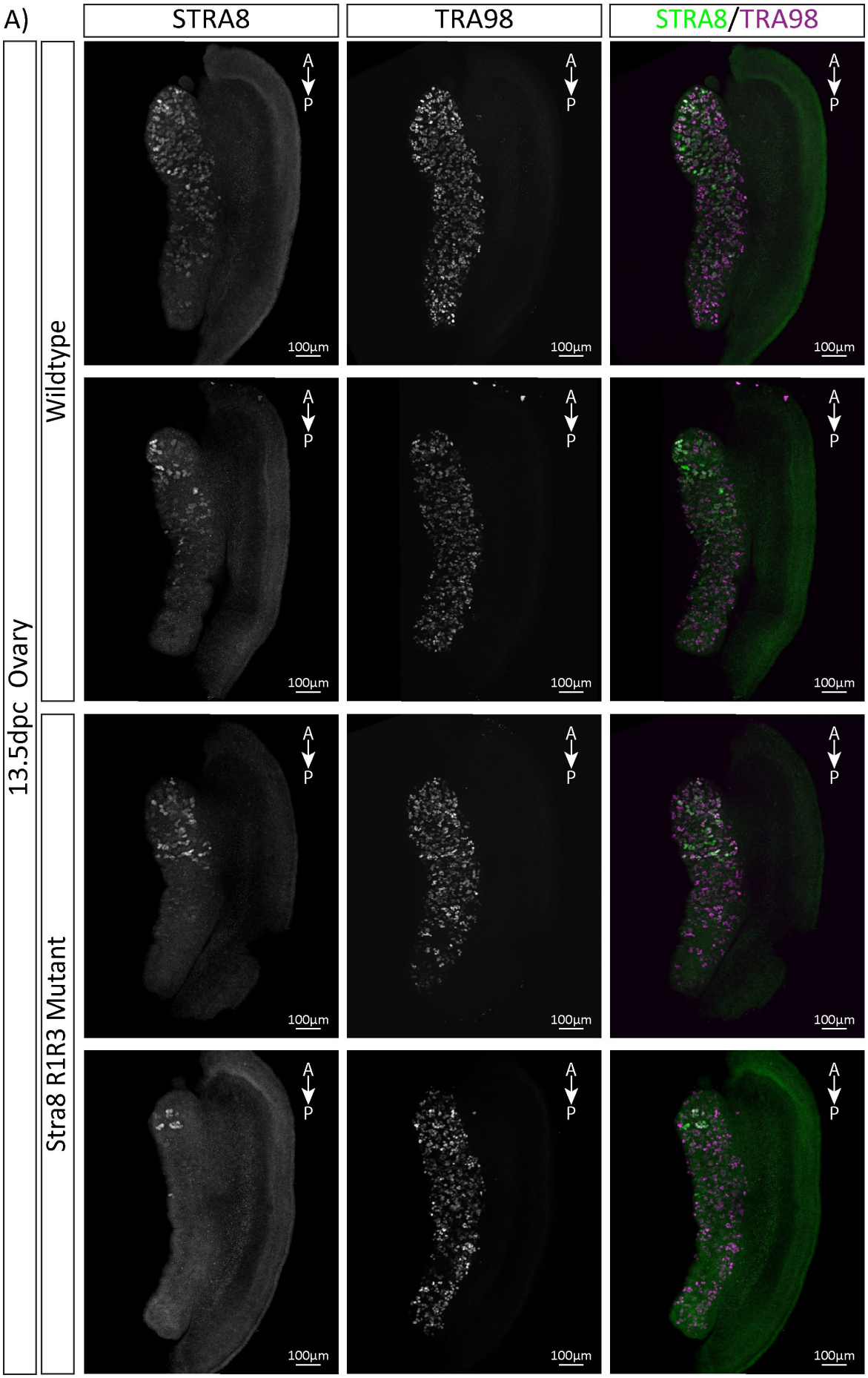

Figure S7: RARE1/3 double mutant retains anterior to posterior wave of STRA8 expression.

Two representative images of whole mount immunofluorescence for STRA8 shows that the anterior to posterior pattern of STRA8 expression see in wildtype ovaries (upper panels) is maintained in RARE1/3 double mutant (lower panels).

Figure S8

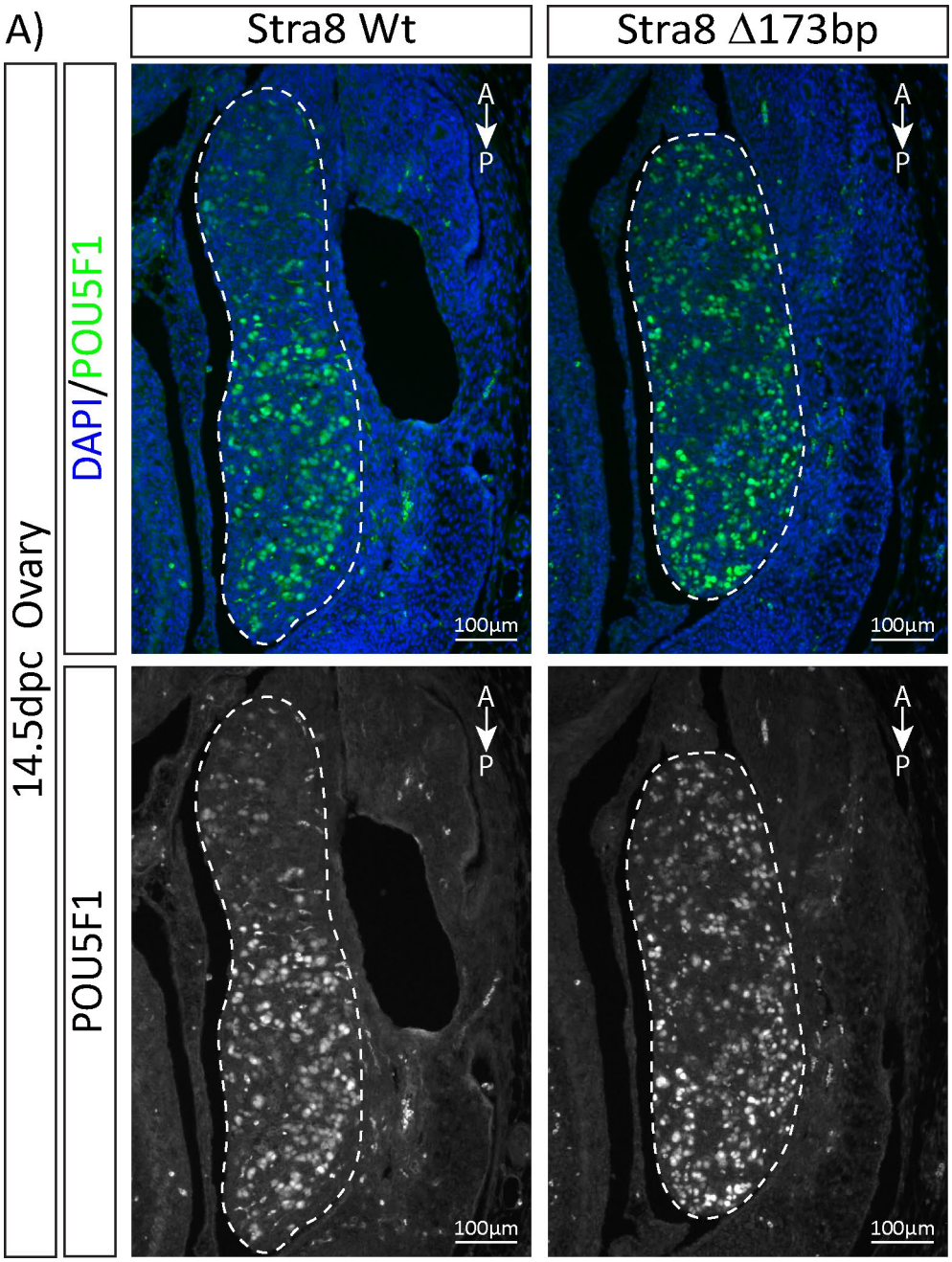

Figure S8: Retention of POU5F1 (a.k.a. OCT4) in Δ173bp mutant ovaries.

Whole mount immunofluoroscence analysis shows the depletion of POU5F1 characteristic at the anterior end of wildtype 14.5 dpc ovaries. This was not observed in a homozygous Δ173bp littermate, where POU5F1 expression is maintained along the entire length of the ovary. This correlates with the retention of *Pou5f1* expression detected by qRT-PCR (Fig. 5B; Fig. S6D).

Figure S9

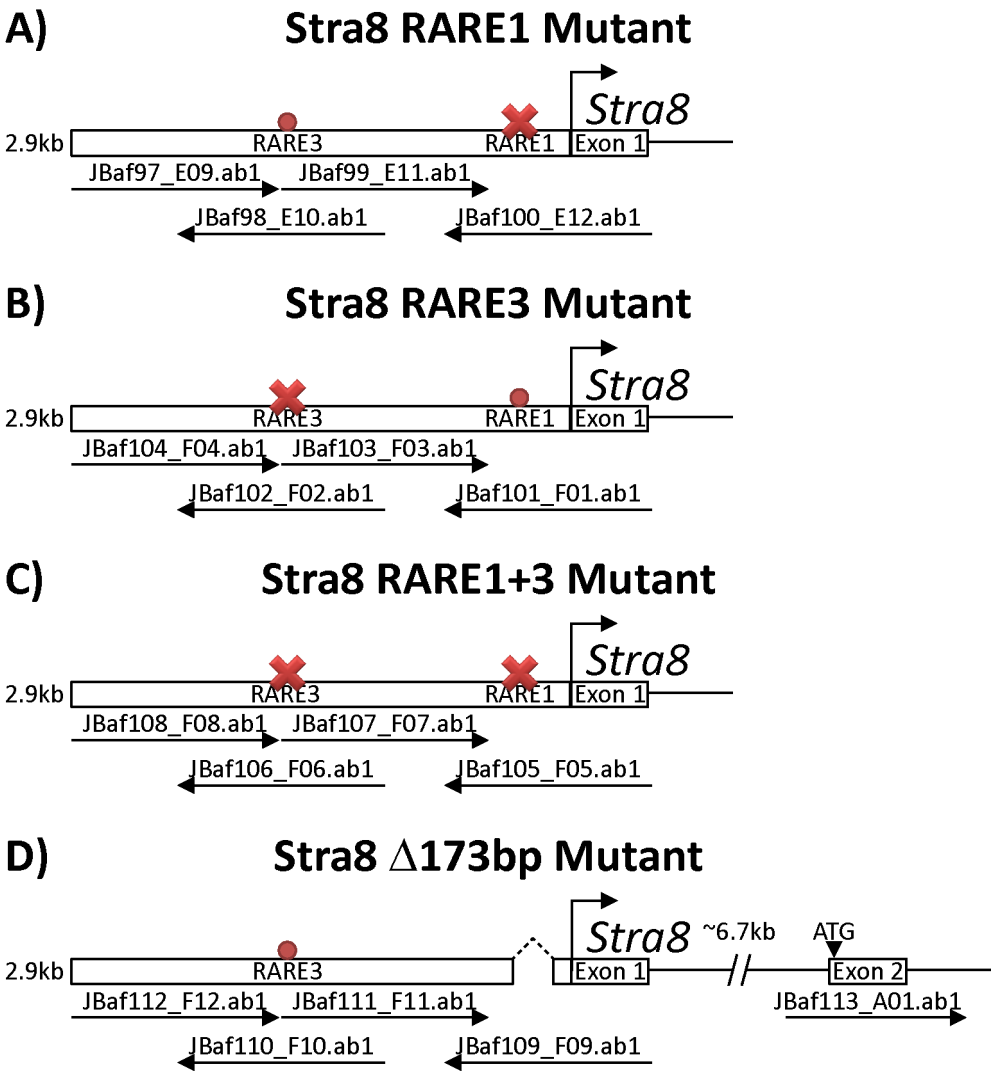

Figure S9: Sequencing coverage of RARE1, RARE3, RARE1+3 and Δ173bp mutant alleles

A-C) 2.9kb promoter and Exon 1 of RARE1, RARE3 and RARE1+3 was cloned and completely sequenced, confirming that only the intended RAREs were mutated. Full overlapping coverage was achieved using 4 primers; reads are as indicated by the black arrows under the diagram of each promoter. D) In addition to sequencing the promoter and Exon 1, the entirety of Exon 2 and flanking intronic sequences were also sequenced for the Δ173bp allele. Exon 2 contains the ATG transcription start site. We confirmed exon 2 to be mutation free, suggesting that it is unlikely that a null allele was inadvertently generated by mutation at that position. All sequencing chromatograms are avaliable as Data S1 (https://doi.org/10.6084/m9.figshare.13506966.v1).

Supplementary Tables

Table S1: Sequences of oligonucleotides used for PCR amplification of genetic sequences, genotyping and SYBR-based qRT-PCR.

Name	Sequence	Used For
2.9kbStra8_F	TCTCGAGCCTTTAGACCCCAGAGC	Amplification of ~2.9 kb *Stra8* promoter
Stra8_R	GACTGCCCGTCGCAGAATAAGAAG	
Stra8_Fw2	TGATTGGTTCGCAGCCTGGG	Genotyping for Stra8-eGFP Transgene
eGFP_Rv1	CGTCGCCGTCCAGCTCGACCAG	
Col1a1-Geno7	CCCAGCTTCACCAGTTCAAT	Genotyping for *Col1a1* Targeting
Col1a1-Geno8	TCATCAAGGAAACCCTGGAC	
GFP_F	GCAGAAGAACGGCATCAAGGTG	GFP qRT-PCR Primers
GFP_R	CTGGGTGCTCAGGTAGTGGTTGTC	
DDX4_F	CAGGAATGCCATCAAAGGAACAAC	DDX4 qRT-PCR Primers
DDX4_R	CCCAACAGCGACAAACAAGTAACTG	

Table S2: Oligonucleotides sequences used for site directed mutagenesis of RARE1, RARE3 and DMRT1 binding sites on *Stra8* promoter constructs for *in vitro* luciferase assays.

Name	Oligo Sequence	Used For
RARE1_ssODN	GCTCCTCTATATCTCAAGAGAAAG TTATAGGTGGCATTGCCCTGGTTG AGGGGTGTAAGAACTGGCGCTAGC CGCCTGGATGGTCGACAAAATTTT TCTTGCTCCTTCCACACCCTCTTGC AACCTGTGGCAAGTTGTTACAATG TTTTCACCAATGTCCACGCTCCCCA TTGGCGCCCCACCATG	Mutation of RARE1 binding site (mutated nucleotides are underlined) RARE1 GGGTGAAAAGGTCA Mutated GTCGACAAAATTTT
Stra8_mutRARE3_antisense	CTTTGTCTTGGAGAGCCTTGTCCTG TCGACAAATTTAATGTGGAGGTTT GCAAACTTTG	Mutation of RARE3 binding site (mutated nucleotides are underlined) RARE3 TCCTCACAGGTCA Mutated TAAATTTGTCGAC
Stra8_mutDMRT1_antisense	GGCGCCAATGGGGAGCGTGGACAT TGGTGAGGCGCGCCGGATCCCTTG CCACAGGTTGC	Mutation of DMRT1 binding site (mutated nucleotides are underlined) DMRT1 TTGTTACAATGTTTT Mutated GGATCCGGCGCGCCT

Table S3: Oligonucleotides sequences used for the generation of CRISPR/Cas9 reagents to target mutations of RARE1 and RARE3 *in vivo*.

Name	Oligo Sequence	Used For
RARE1 -top	CACCGGCGCTAGCCGCCTGGAT	Annealed and inserted into PX330 to generate RARE1 sgRNA template for IVT
RARE1 -bottom	AAACATCCAGGCGGCTAGCGCC	
RARE1_ssODN	GCTCCTCTATATCTCAAGAGAAAG TTATAGGTGGCATTGCCCTGGTTG AGGGGTGTAAGAACTGGCGCTAGC CGCCTGGATGGTCGACAAAATTTT TCTTGCTCCTTCCACACCCTCTTGC AACCTGTGGCAAGTTGTTACAATG TTTTCACCAATGTCCACGCTCCCCA TTGGCGCCCCACCATG	HDR template for generating CRISPR/Cas9 mediated RARE1 mutation
RARE3_sgRNAF	AATACGACTCACTATAGGGGCAAA CCTCCACATTCCTCACGTTTTAGAG CTAGAAATAGCAAGTTAAAATAAG GCTAGTC	Annealed and filled to generate template for RARE3 sgRNA IVT.
Chimeric_sgRNA_R	TAAAAAAGCACCGACTCGGTGCCA CTTTTTCAAGTTGATAACGGACTA GCCTTATTTTAACTTGCTATTTCTA GCTCTAAAAC	
RARE3_ssODN	ACTAAATTAAAGGCTGAGACCTGT CAGAGGTCAAAGTTTGCAAACCTC CACATTAAATTTGTCGACAGGACA AGGCTCTCCAAGACAAAGGTTCAC AGTTTCAGTACCCGTTCTGCACCC	HDR template for generating CRISPR/Cas9 mediated RARE3 mutation

Table S4: Breeding Statistics for Δ173 heterozygous and homozygous mice

Number of breeders	Average Days Setup (S.D.)	Average Days to birth of 1st litter (S.D.)	Average number of litters (S.D.)	Average litter size (S.D.)
16 Heterozygous (11M, 5F)	173.55 (87.75)*	29.45 (12.81)	4.36 (2.31)	7.11 (1.52)
8 Homozygous (4M, 4F)	82.75 (5.02)	N/A	0	0

*Statistics extracted from breeding colony: breeders were allowed to breed for longer than was done for the homozygous animals. S.D. = standard deviation.